REGISTERED No. M. 3121

UNIVERSITY
OF MICHIGAN
MAR 21 1955
PHYSICS
LIBRARY

PROCEEDINGS
OF THE
INDIAN ACADEMY
OF SCIENCES

VOL. XLI] *SECTION A* [No. 1

JANUARY 1955

Price Rs. 2 or 3 Sh. *Annual Subscription Rs. 18*

PRINTED AT THE BANGALORE PRESS, BANGALORE CITY, BY C. VASUDEVA RAO,
SUPERINTENDENT AND PUBLISHED BY THE INDIAN ACADEMY OF
SCIENCES, BANGALORE

ON THE OPTICAL BEHAVIOUR OF CRYPTO-CRYSTALLINE QUARTZ

By Sir C. V. Raman and A. Jayaraman

(*Memoir No. 64 of the Raman Research Institute, Bangalore*)

1. Introduction

The present paper may be regarded as a sequel to two earlier communications[1, 2] by the present authors in these *Proceedings* which dealt with the structure and optical behaviour of iridescent agate and of the commoner forms of chalcedony. We have felt it desirable to supplement those two papers by a somewhat fuller description and discussion of the optical phenomena presented by these materials. Of particular interest is the property exhibited by the relatively more transparent specimens of chalcedony of polarising the light transmitted by them perfectly. This phenomenon is illustrated in a striking manner by Figs. 1 and 2 reproduced in Plate I; these are photographs of the entrance to the building of this Institute and of the landscape beyond as viewed through a plate of chalcedony about a millimetre thick on which was superposed a polaroid sheet. In Fig. 1, the building and landscape are seen clearly, while in Fig. 2 they are completely smudged out. In the former case, the polaroid had its vibration direction parallel to the fibres of quartz composing the chalcedony, while in the latter the vibration direction of the polaroid was transverse to the fibres. Similar effects are exhibited by Figs. 3 and 4 which are photographs of a sodium vapour lamp recorded in analogous circumstances. Polarisation effects of the same nature are also observed in the transmitted light which appears along with the diffraction spectra exhibited by iridescent agate. We shall return to these phenomena later in the paper.

An interesting and important aspect of the present subject is the close correlation which exists between the optical phenomena and the structure of the materials as revealed by X-ray diffraction studies. Large variations in structure are evident from the series of twelve X-ray diagrams reproduced in Plate III and Plate IV, and they correspond to striking differences in optical behaviour.

2. Some Theoretical Considerations

The phenomena exhibited by chalcedony and agate in varied circumstances are best elucidated by first considering a few idealised cases in the

light of a simplified geometric theory. We may assume the material to be composed of crystallites of quartz completely filling its volume. Had the material been optically isotropic, light would freely pass through the polycrystalline aggregate. Actually, the birefringence of the quartz is sufficient to ensure the total diffusion of the light in its passage through a plate of the material as a result of the refractions at the inter-crystalline boundaries, provided that the optic orientation of the crystallites is assumed to be entirely at random. A distant source of light viewed through such a plate would be invisible; a diffuse halo of light would be observed in the same general direction which would exhibit no observable polarisation even if the incident light be fully polarised.

It is evident from the foregoing that a preferred orientation of the crystallites is a *sine qua non* in order that any observable fraction of the light be regularly transmitted through the material. Indeed, the geometric theory demands a perfectly ordered orientation of the crystallites for an optical image of a light source to be visible through a plate of the substance. The maximum transmission would occur if the crystallites were so arranged that the principal optical axis of quartz, *viz.*, the *c*-axis were aligned in perfect parallelism for all of them. Actually, we have not encountered a case of this kind in our studies, though an approximation to it has been noticed in some specimens of fibrous quartz.[3] On the other hand, chalcedony consisting of crystallites of quartz with some direction perpendicular to the *c*-axis such as $[1\bar{1}00]$ or $[11\bar{2}0]$ set more or less perfectly parallel for all of them appears to be fairly common. In such an arrangement, the orientation of the *c*-axis would vary from one crystallite to another.

3. THE X-RAY DIFFRACTION PATTERNS

The foregoing remarks are illustrated by Figs. 1 to 6 in Plate III and Figs. 1 to 6 in Plate IV. Fig. 1 in Plate III is the X-ray diffraction pattern of agate recorded for a region exhibiting brilliant iridescence and using unfiltered MO radiation. It is seen that the pattern is a fibre diagram in which the crystallites are orientated with fair precision in a direction parallel to the *a*-axis of quartz, while their *c*-axes are orientated in all possible directions perpendicular thereto. Fig. 2 in the same Plate was also recorded with another piece of agate exhibiting iridescence; it shows a lesser precision in the orientation of the crystallites but which is of the same kind. Still less well defined is the orientation of the crystallites of the same nature seen in Fig. 3. This was obtained with a polished plate of chalcedony exhibiting a fair measure of transparency.

Fig. 4 in Plate III was obtained with a polished plate of chalcedony which was remarkably transparent, being in fact the one with which the photographs reproduced in Plate I were obtained. It can be interpreted as a fibre diagram in which the fibres are parallel to the [1$\bar{1}$00] direction, while the *c*-axis takes all possible orientations perpendicular thereto. A clear indication of the same type of fibering is illustrated in Fig. 5 which was recorded with a translucent specimen of coloured agate. Fig. 6 in Plate III was recorded with the same iridescent agate as Fig. 1 but in a region exhibiting no conspicuous banding or iridescence. The figure does exhibit preferred orientation of the crystallites but not of a sharply defined character, which appears to be intermediate between the types illustrated in Figs. 1 and Fig. 5 in Plate III.

Fig. 1 in Plate IV is an X-ray diagram of powdered quartz. The remaining five figures in the Plate are diagrams of chalcedony and agate in which hardly any preferred orientation is to be noticed. Fig. 6 in Plate IV which almost resembles Fig. 1 in the same Plate was recorded with a chip of chalcedony exhibiting little transparency.

4. Polarisation of the Transmitted Light

We may now consider the case of a plate of chalcedony assumed to be cut in such a manner that the *a*-axes of the crystallites are all parallel to each other and to the surface of the plate. If light be normally incident on such a plate with its vibration direction parallel to the common direction of the *a*-axes of the crystallites, it is evident that it would be freely transmitted by the plate. If, on the other hand, the vibration direction of the incident light be transverse to the same common direction, the variation of the direction of the *c*-axis from crystallite to crystallite would result in the light being refracted at the inter-crystalline boundaries and hence none of the incident light would be transmitted. The directions in which the light diffused would emerge and the state of its polarisation would both depend upon the orientation of the inter-crystalline boundaries, in other words on the shape of the crystallites. If the latter are elongated cylinders or fibres with their length parallel to their *a*-axes, the light diffused would appear as a fan of refracted rays lying in a plane perpendicular to the direction of the fibres: it would also be completely polarised with the vibration direction transverse to the fibres.

5. Diffraction Phenomena

Though geometric considerations of the kind set forth above suffice to give a qualitative picture of the phenomena, they would not describe completely what is actually observed. The light rays deviated by the individual

fibres would evidently be in a position to interfere with each other. Hence the fan of rays diffused by the plate should properly be regarded as due to the passage of light through an irregular phase-change grating. This would diffract the light in various directions transverse to the fibres. Further, if the length of the individual fibre were not great enough, light would also be spread out by diffraction to some extent in other directions.

The importance of the part which diffraction plays in the optical phenomena is most strikingly evident in the case of iridescent agate. As has been already remarked and illustrated in our earlier paper on the subject, the light *regularly* transmitted by iridescent agate is perfectly polarised, the only difference between the iridescent and non-iridescent regions being that the intensity of transmission is greatly enfeebled in the former by reason of the radiation energy being copiously diffracted in other directions. It is highly significant that these diffracted radiations are neither wholly nor even partly concentrated in specific directions as would be the case with ordinary gratings. The diffracted radiations in fact appear as elongated streaks, and that they are well-defined streaks is made evident by using a monochromatic light source and selected regions on the agate where the spacings are most regular. No image of the source is however seen except at the centre of the spectrum of zero order. The diffraction streaks exhibit a partial polarisation which is in the same sense as the polarisation of the regularly transmitted light near their central regions but in the opposite sense further out in the streaks on either side. This situation will be evident from the photographs reproduced as Figs. 3 and 4 in Plate II exhibiting respectively the two components of polarisation of the diffraction pattern observed with sodium light.

The explanation of the facts stated above leads us directly to the solution of the problem of the nature of the laminations in iridescent agate which we shall now proceed to consider.

6. THE STRUCTURE OF IRIDESCENT AGATE

We shall assume that the fibres of quartz in the iridescent layers of agate have all a common direction and also a common optic orientation. That this assumption is substantially correct is evident from the complete polarisation of the light regularly transmitted through the iridescent layers and is further confirmed by the X-ray diffraction studies to which we have already referred. What then is the nature of the periodicity that gives rise to the diffraction spectra? We have already remarked that the diffraction streaks observed with fibrous chalcedony are a consequence of the varying orientation of the *c*-axis from fibre to fibre. Hence, the natural interpretation of the observed optical behaviour of the iridescent regions is that the orienta-

tion of the *c*-axis is periodic along the length of each individual fibre. In fact, one is led to that interpretation by a simple process of exclusion. What is actually observed is a diffraction of light by a phase-change grating which is irregular along the plane of the laminations but is regular and periodic in the perpendicular direction, in other words, *along* the length of the fibres. A periodicity in the orientation of the *c*-axis along the length of each fibre is just what is required to give rise to such a situation. We remark that since the change of phase affects only the vibration transverse to the fibres, it would give rise to diffracted beams polarised in that sense. But, as we have already seen, such beams are not regularly transmitted but are diffused into a fan of rays. The non-appearance of any optical images of the source in the spectra is thus explained. We do indeed observe in the spectra a region of enhanced intensity near their centres which is partially polarised in the same sense as the regularly transmitted light. But this is evidently a secondary effect arising by reason of our assumption of a perfectly orientated fibre structure being an idealisation which differs noticeably from the actual situation.

7. The Moiré Patterns of Iridescent Agate

A striking confirmation of the conclusions set forth above is furnished by a study of the moiré patterns exhibited by the iridescent regions. These patterns are readily observed by merely holding up the plate against a source of light and viewing it through a magnifier. They are only seen in the regions displaying iridescence. Small tilts of the plate produce large changes in the configuration of the patterns, thereby indicating their origin, which is that the laminations in the material at different depths are not in perfect register. The introduction of a polaroid between the iridescent agate and the observer's eye produces a remarkable change in the moiré pattern. When the vibration direction of the polaroid is transverse to the laminations, in other words parallel to the fibre direction, the moiré pattern disappears practically completely. If, on the other hand, the polaroid is set with its vibration direction parallel to the laminations and hence transverse to the fibres, the moiré pattern becomes extremely conspicuous. These effects are shown in Figs. 1 and 2 in Plate II.

The interpretation of the facts is obvious, *viz.*, that the periodic changes of phase produced by the grating which progressively transform themselves to periodic variations of amplitude are operative only in respect of the optical vibrations transverse to the fibre length. This is precisely the result which would ensue as a consequence of a periodic change in the orientation of the *c*-axis along the length of each individual fibre.

Neither the observed diffraction effects nor the behaviour of the moiré patterns could be reconciled with a periodicity of structure due to a rhythmic segregation of opal as has been suggested in a recent paper[4] on iridescent agate which has been brought to our notice. Further, as has been shown elsewhere[5] by us, the opal that is actually found associated with agate is identifiable with α-cristobalite. This exhibits a very intense X-ray diffraction ring with a spacing of 4·03 A.U. Not even a trace of a ring with such a spacing is to be observed in the X-ray diagram recorded by us in the strongly iridescent regions of our agate specimens.

SUMMARY

The polarisation of the light regularly transmitted by fibrous chalcedony and the character of the diffraction spectra exhibited by iridescent agate are described and discussed. It is shown that the phenomena point conclusively to the laminations in iridescent agate responsible for the diffraction effects being a consequence of the periodic orientation of the *c*-axis of quartz along the length of the fibres. Photographs illustrative of the optical effects and of the X-ray diffraction patterns of the materials are reproduced.

REFERENCES

1. C. V. Raman and A. Jayaraman .. *Proc. Ind. Acad. Sci.*, 1953, **38A**, 199.
2. A. Jayaraman .. *Ibid.*, 1953, **38A**, 441.
3. C. V. Raman and A. Jayaraman .. *Ibid.*, 1954, **40A**, 107.
4. F. T. Jones .. *Amer. Mineral.*, 1952, **37**, 578.
5. C. V. Raman and A. Jayaraman .. *Proc. Ind. Acad. Sci.*, 1953, **38A**, 343.

FIG. 1

FIG. 2

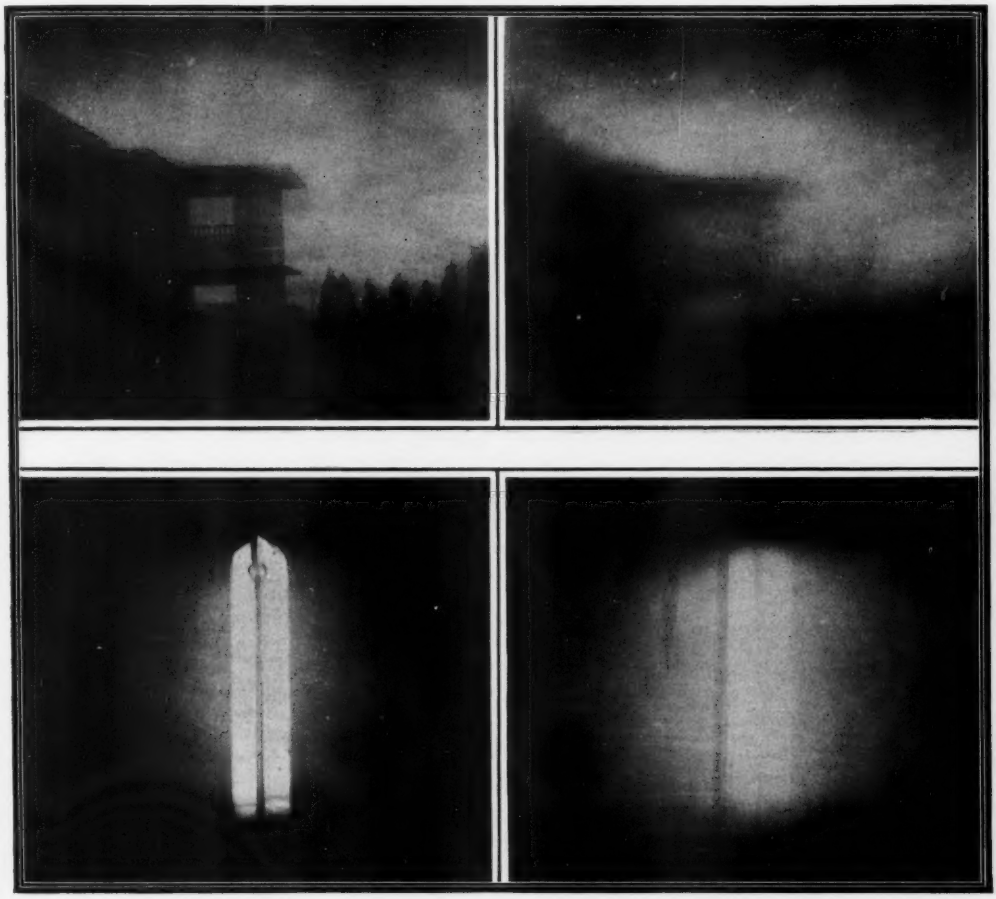

FIG. 3

FIG. 4

Polarisation of Light by Chalcedony

FIG. 1

FIG. 2

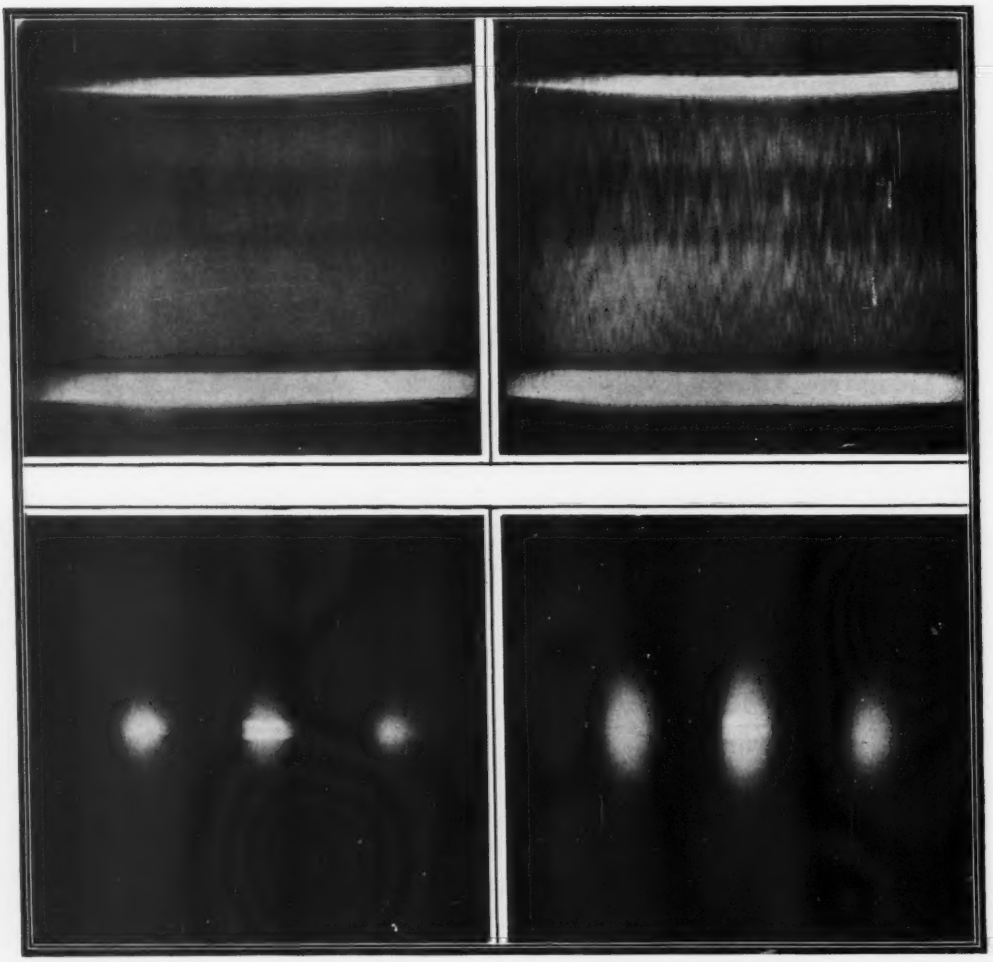

FIG. 3

FIG. 4

Polarisation of Light by Iridescent Agate

FIG. 1

FIG. 4

FIG. 2

FIG. 5

FIG. 3

FIG. 6

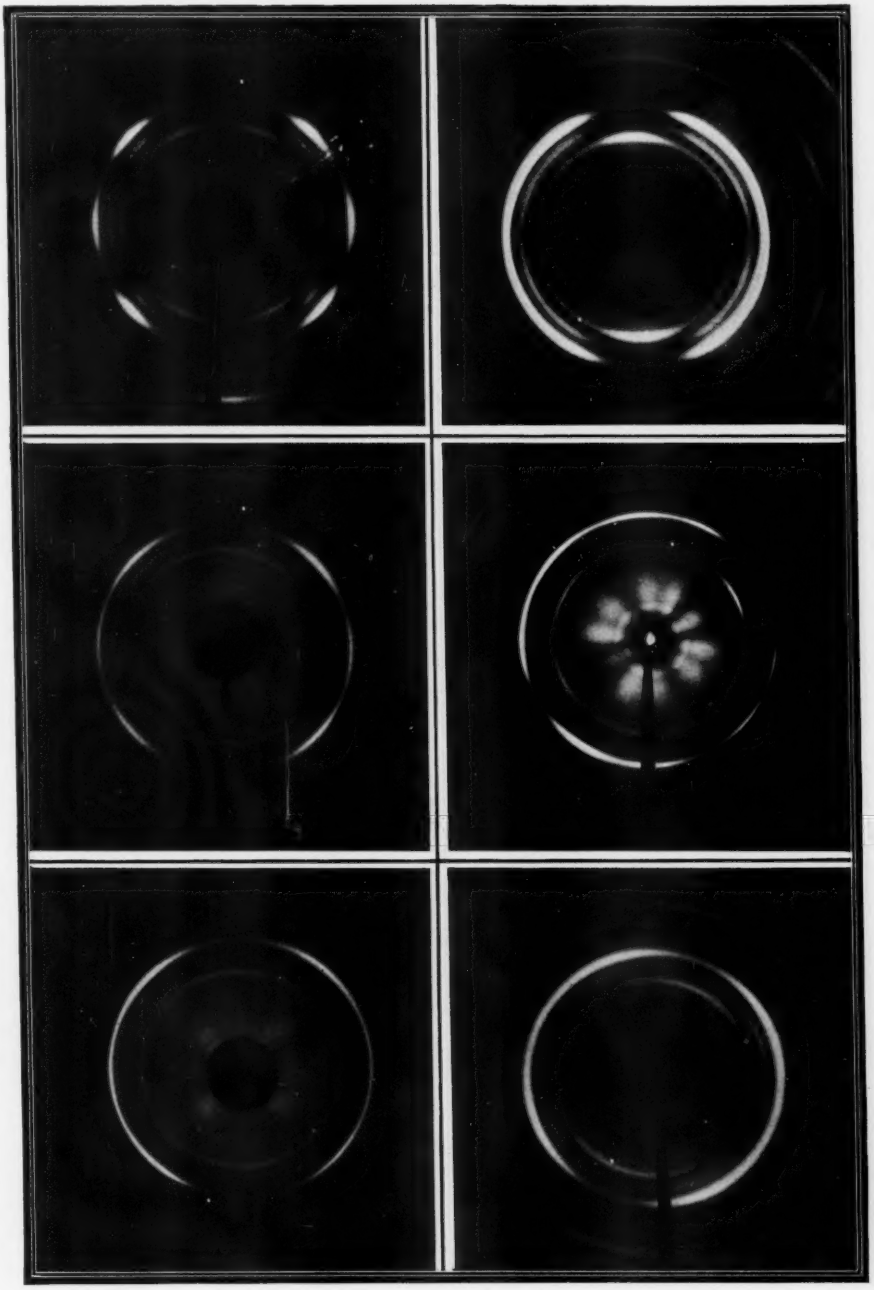

X-Ray Diffraction Patterns

FIG. 1

FIG. 4

FIG. 2

FIG. 5

FIG. 3

FIG. 6

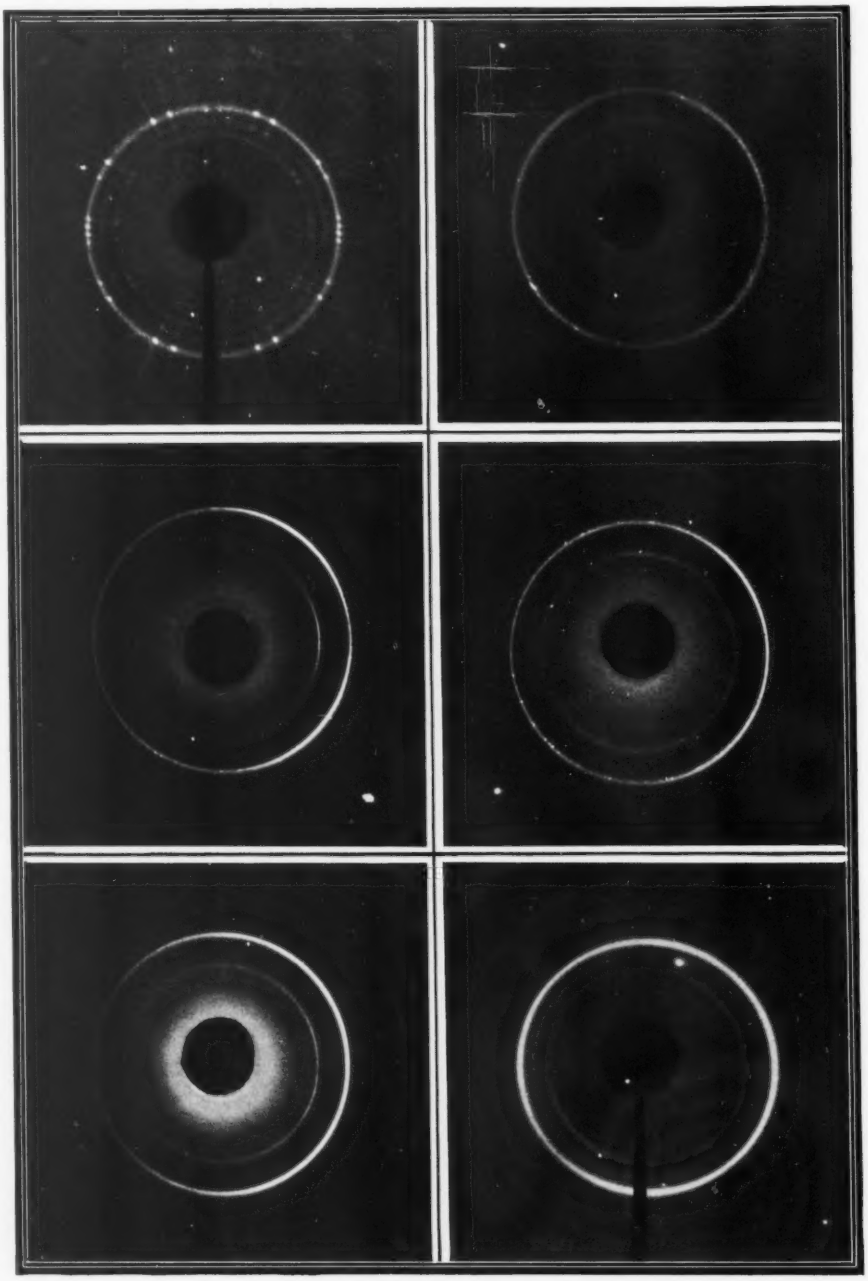

X-Ray Diffraction Patterns

RAMAN SPECTRA OF BORAX, KERNITE AND COLEMANITE

By D. Krishnamurti

(*Memoir No. 65 from the Raman Research Institute, Bangalore*)

Received January 8, 1955

(Communicated by Sir C. V. Raman)

1. Introduction

The Raman effect in boric acid and its derivatives and the glasses associated with them has been studied by several investigators. A brief summary of the results appears in Hibben's treatise on "The Raman Effect and its Chemical Applications". The Raman spectrum of borax ($Na_2B_4O_7 \cdot 10H_2O$) has been observed by Nielsen (*vide* Hibben's treatise, p. 433) and has been found to consist of seven frequencies at 578 (1), 853 (1), 891 (1), 942 (1), 3340 (1), 3455 (1) and 3574 (1) cm.$^{-1}$ Kernite ($Na_2B_4O_7 \cdot 4H_2O$) was investigated by Hibben (1937) who reports ten frequencies at 500 (2), 575 (0), 735 (3), 850 (0), 934 (6), 1100 (?), 3269 (2), 3343 (3), 3425 (2) and 3552 (10) cm.$^{-1}$ Gross and Vuks have reported in borax glass diffuse bands in the regions 430–535 (0), 950–1000 (0), 1077–1127 (0), and 1310–1520 (0) and a strong line at 760 (5) cm.$^{-1}$ It is rather surprising that Nielsen did not notice any shift corresponding to 760 cm.$^{-1}$ in borax. The Raman spectrum of colemanite ($Ca_2B_6O_{11} \cdot 5H_2O$) has not so far been investigated. In view of the interest attached to these substances and the fact that the low frequency spectra of these have not so far been reported, it appeared to be desirable to investigate the spectra of these substances. The paper reports the findings from the study.

2. Experimental Details

The Raman spectra were recorded with a Hilger medium quartz spectrograph having a dispersion of 140 cm.$^{-1}$ per mm. in the λ 2536·5 region. A quartz mercury arc of the sealed type with mercury pools as electrodes was immersed in a trough of running water and an electromagnet was used to deflect the discharge towards the top wall of the arc. With a current of 3 amperes this arrangement constituted to give an intense source of λ 2536·5. The crystals were kept quite close to the arc and the scattered radiations from the crystal were focussed on the slit of the spectrograph with a quartz condenser. Two mercury dishes were placed inside the spectrograph one at the collimator side and the other at the plate-holder side. The mercury

vapour inside the spectrograph was sufficient to effectively suppress the exciting λ 2536·5 radiation so that in the spectrograms obtained, it appeared much feebler than its satellite λ 2534·8.

The crystals of borax which were rather small were efflorescent and as such fresh crystals had to be used periodically. A large specimen of kernite in the form of a thick plate was available and it was possible to record in this case a very intense spectrum. The specimen of colemanite which was somewhat smaller in size had well-developed faces forming a pyramid, but was intensely luminescent under near ultraviolet radiations. Kernite was also slightly luminescent. This fact coupled with the feeble scattering in these crystals made it impossible to record their Raman spectra with λ 4358 in the visible. In the ultraviolet region on the other hand, because of the large scattering power of the λ 2536·5 radiations the luminescence did not overpower the scattering. With a slit width of 0·045 mm. and an exposure of the order of 16 hours it was possible to obtain reasonably intense spectrograms. The complete spectrum of borax could not be obtained since the crystals grown by the method of slow evaporation were small.

3. RESULTS

Figures 1 (*b*), 1 (*c*), 1 (*d*) in the accompanying plate reproduce the Raman spectra of borax, kernite and colemanite respectively while Figs. 1 (*a*), and 1 (*e*) reproduce the spectrum of the mercury arc for comparison. In some cases the lines were rather weak and diffuse or else were partially overlapping on a mercury line and the frequency shifts of these were estimated by comparison with the position of the iron arc lines.

Borax exhibits seven lines at 159 (*w*), 349 (*w*), 458 (*m*), 572 (*m*), 753 (*w*), 847 (*v. w*), and 944 (*s*) cm.$^{-1}$ and four bands due to water at 3325, 3444, 3500 and 3577 cm.$^{-1}$ Of these the frequency at 3577 cm.$^{-1}$ is very intense and comparatively sharp. Nielsen has not reported the faint band at 3500 cm.$^{-1}$ The line reported at 891 cm.$^{-1}$ by Nielsen has not been recorded and only a trace of a line could be noticed at about 847 cm.$^{-1}$

Table I presents the data in the case of kernite and colemanite and the general correspondence between the two spectra can be noticed. In the case of colemanite, the intense frequency shift at 940 cm.$^{-1}$ observed in kernite and borax has not been recorded.

The spectrum due to water shows striking variations in its structure and in particular the frequency shift of the sharp and intense band corresponding to the hydroxyl group changes from 3552 cm.$^{-1}$ in kernite to 3577 cm.$^{-1}$ in borax and to 3605 cm.$^{-1}$ in colemanite.

TABLE I

Frequency Shifts

Kernite cm.$^{-1}$	Colemanite cm.$^{-1}$	Kernite cm.$^{-1}$	Colemanite cm.$^{-1}$
55 *s.*	..	806 *m.*	786 *w.*
82 *v.s.*	..	846 *m.*	~ 870 *w.*
104 *s.*	95 *v.s.*	932 *v.s.*	..
127 *s.*	..	951 *v.w.*	~ 982 *v.w.*
152 *w.*	148 *m.*	~ 1028 *m.*	..
184 *s.*	181 *s.*	1087 *s.*	1078 *m.*
~ 215 *v.w.*	223 *m.*	1135 *m.*	~ 1150 *w.*
258 *s.*	251 *m.*	1321 *s*	~ 1252 *w.*
		1375 *v.w.*	~ 1310 *w.*
315 *w.*	318 *s.*	1448 *w.*	..
346 *w.*	..	~ 1480 *v.w.*	..
371 ~ 391 *b.m.*	..	~ 3000 *s.*	..
426 *v.w.*	..	3248 *s.*	~ 3310 *s.*
459 *m.*	~ 450 *v.w.*	~ 3305 *s.*	..
498 *v.s.*	~ 490 *v.w.*	~ 3360 *s.*	..
541 ? *v.w.*	538 *s.*	~ 3425 *s.*	
562 *w.*	565 *s.*	3548 *v.s.*	~ 3520 *s.*
..	670 *s.*	..	3605 *v.s.*
739 *v.s.*	745 *v.s.*	..	

s. strong; *w.* weak; *m.* moderate; *v.s.* very strong; *v.w.* very weak; *b.* broad. ~ value of frequencies estimated by comparison with position of adjacent iron arc lines.

4. DISCUSSION

Borax, kernite and colemanite crystallize in the holohedral class of the monoclinic system and have been assigned to the space groups C2/c, P2/c and $P2_1/a$ respectively [*Structure Reports*, Vol. 11, pp. 428–31 and Christ, Clark and Evans (1954)]. The existence of a centre of symmetry in all these cases precludes the possibility of observing any of these lines in infra-red absorption also. Reference to the literature has revealed that no infra-red absorption studies have so far been made with borax and kernite. However, the infra-red spectrum of metallic orthoborates have been studied by Sen and Sen Gupta (1935) in the near infra-red by transmission, by Parodi (1937) in the far infra-red both by reflection and transmission, and lately extensively by Lecomte and Duval (1952) in the near infra-red by transmission. For calcium borate [$Ca_3(BO_3)_2$] they observe maxima at 676, 734, 784, 814, 876, 922, 1000, 1100, 1168, 1340 and 1412 cm.$^{-1}$ Parodi reports in the far infra-red for calcium borate frequencies at 365, 325, 250 and 192 cm.$^{-1}$

Lecomte and Duval have discussed in detail the origin of such a large number of frequencies since an ordinary planar BO_3 group should possess only four vibration frequencies. They attribute the large number of frequencies to the coupling of BO_3 groups and they calculate that two such groups coupled would give rise to eighteen vibration frequencies, the totally symmetric valence vibration frequency being in the region 909–934 cm.$^{-1}$ The structure of borax is reported to consist of BO_3 triangles sharing common vertices and forming an infinite chain along the *c*-axis consisting of B_4O_7 rings. Kernite on the other hand, is supposed to be made up of B_3O_6 rings formed by three BO_3 triangles sharing vertices, coupled together by B_2O_3 groups from two BO_3 triangles, thus forming an infinite B_4O_7 zig-zag chain along the *b*-axis. The vibrations of such a structure consisting of coupled BO_3 triangles would give rise to a large number of frequencies and it is possible here to identify only the frequency at 932 cm.$^{-1}$ in kernite and at 944 cm.$^{-1}$ in borax as due to the valence oscillation of the borons and oxygens.

The structure of colemanite recently determined by Christ, Clark and Evans (1954) is reported to consist of infinite boron-oxygen chains running parallel to the *a*-axis, the chain element being constituted by a BO_3 triangle and two BO_4 tetrahedra forming a ring, the chain element having the composition $[B_3O_4(OH)_3]^{-2}$. It has also been found by them that the B—O bond lengths in the tetrahedra are larger than the bond lengths in the triangles. Again, since colemanite also possesses a centre of symmetry no correspondence could be normally expected between the data from Raman and infra-red spectra. But the studies of Coblentz (1906) on the infra-red reflection spectrum of colemanite reveal the existence of frequencies at 1370, 1316 (?), 1064, 943 and 893 cm.$^{-1}$, which have nearly corresponding frequencies at 1310, 1078, 982 and 870 cm.$^{-1}$ in Raman effect. It is rather surprising that there is no Raman frequency in colemanite corresponding to the 940 cm.$^{-1}$ shift in borax and kernite. If the vibrating structure in colemanite consists of BO_3 triangles coupled to BO_4 tetrahedra having different bond lengths, as has been suggested by Christ, Clark and Evans, the principal vibration frequency of this system might be different from what has been observed in kernite and borax.

The existence of the O—H group in the chain element of colemanite is consistent with the observation in Raman effect of an intense and sharp band at 3605 cm.$^{-1}$ and corresponding to the hydroxyl group frequency. Though the reported structures of kernite and borax do not contemplate the existence of the hydroxyl group in them, the observation of sharp and intense bands at 3548 and 3577 cm.$^{-1}$ in their respective Raman spectra indicate the existence

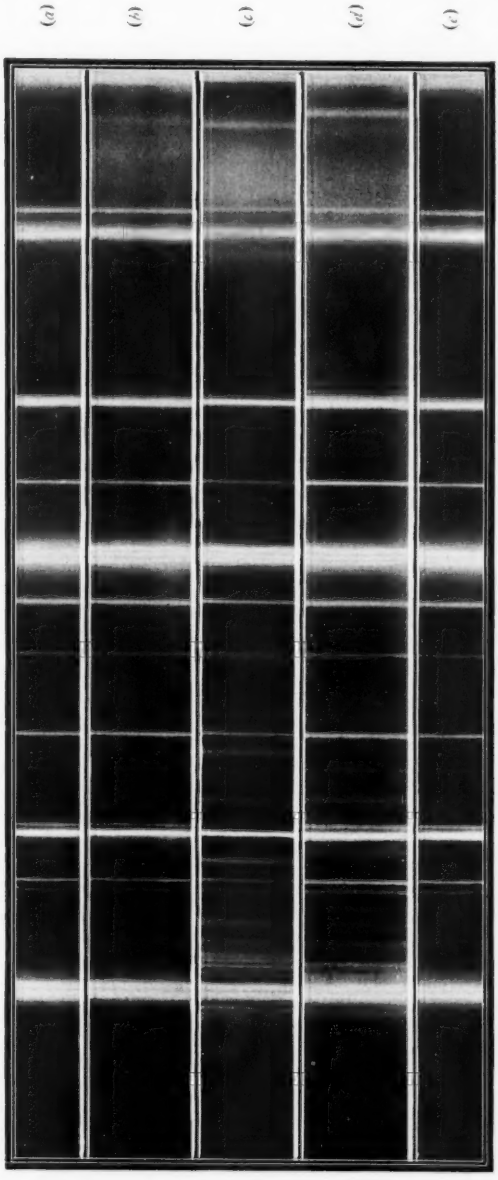

FIG. 1. Raman Spectra of Borax, Kernite and Colemanite
(*a*) Mercury arc. (*b*) Borax. (*c*) Kernite. (*d*) Colemanite. (*e*) Mercury arc.

of such groups in their structures. It is hoped that polarisation and orientation studies would help towards a more detailed analysis of the observed spectra of these chain structures.

The author's grateful thanks are due to Prof. Sir C. V. Raman, F.R.S., N.L., for suggesting this investigation and the encouraging interest that he took in it.

Summary

The Raman spectra of borax, ($Na_2B_4O_7 \cdot 10H_2O$), kernite ($Na_2B_4O_7 \cdot 4H_2O$) and colemanite ($Ca_2B_6O_{11} \cdot 5H_2O$) have been investigated using λ 2536·5 as exciting radiation. The spectrum of colemanite is reported for the first time. Many additional lines hitherto unreported have been found in the case of kernite and borax. The spectrum of borax exhibits seven lines, besides four bands due to water of crystallisation while the spectrum of kernite is found to consist of twenty-eight lines and six water bands. Colemanite exhibits nineteen Raman lines, and three bands due to water of crystallization. The observed spectra are discussed in relation to the known structures of the substances.

References

Christ, Clark and Evans .. *Acta. Cryst.*, 1954, **7**, 453.

Coblentz .. *Investigations of Infra-red Spectra*, 1906, Part 4, 85.

Gross and Vuks .. *C.R. Acad. Sci., U.R.S.S.*, 1935, **1**, 214.

Hibben .. *Raman Effect and Its Chemical Applications*, 1939, 430–39.

Lecomte and Duval .. *Bull. Soc. Chim.*, France, 1952, **19**, 101–05.

Parodi .. *C.R. Acad. Sci.*, Paris, 1937, **204**, 1111.

Sen and Sen Gupta .. *Ind. Jour. Phys.*, 1935, **9**, 433.

TRANSMISSION OF ULTRASONICS THROUGH ROCKS

By S. Balakrishna

(From the Physical Laboratories, Osmania University, Hyderabad)

Received December 8, 1954

(Communicated by Dr. S. Bhagavantam, F.A.SC.)

1. Introduction

The elastic properties of rocks which are in the nature of polycrystalline aggregates, are dependent, on the order and arrangement of the crystallites composing the aggregates and also on the closeness of packing; particle size and mineralogical composition. During the last few years, high frequency methods have been widely applied for measuring such properties. That the attenuation and velocity of high frequency sound waves is connected with particle size in solids has been demonstrated by Mason and Mcskimin (1947). Takahashi and Yasusato (1949) studied the theory of propagation of elastic waves in granular substances and observed that sound waves are propagated in sand with only $\frac{1}{3}$ of their velocity in rocks. The author in an earlier paper (1952) observed that transmission of sound in rocks is dependent on granular structure and mineralogical composition. Following this and in the course of a detailed investigation of physical properties of rocks, it has been noticed that there are significant variations in ultrasonic velocities in the same types of rocks taken from different localities. In order to explain these variations, the author has studied the granular structure of some typical rocks under a polarising microscope. The present paper attempts a correlation between the particle size and transmission of sound in monomineralic rocks like quartzites and limestones.

2. Experimental Technique and Results

Using the total internal reflection method described by Krishnamurthi and Balakrishna (1953), longitudinal and torsional ultrasonic velocities are determined in three quartzites and three limestones obtained from different localities. The results are given in Table I.

V_L and V_S in Table I are longitudinal and torsional velocities respectively in metres/sec. and are determined at room temperature and atmospheric pressure. Plate VI gives the microphotographs of the above rock sections obtained with a petrological microscope using polarised light. All pictures are taken at the same magnification, namely, $\times 30$. Figs. 1 *a*, *b* and *c* are

TABLE I

No.	Rock	Locality	Density in gm./c.c.	Grain Size	V_L	V_S
1	Quartzite ..	Khammammet	2·51	0·1 mm.	6621	3400
2	Quartzite ..	Warangal	2·56	0·3 mm.	5610	3030
3	Quartzite ..	Karimnagar	2·54	0·6 mm.	5060	2700
4	Limestone ..	Ramagundam	2·80	Fine	7069	3403
5	Limestone ..	Cuddapah	2·82	Medium	6400	3200
6	Limestone	Vindhya Pradesh	2·81	Coarse	6260	3065

for quartzites 1, 2 and 3 and Figs. 2 *a*, *b* and *c* are for limestones 4, 5 and 6 of Table I.

3. Discussion

In an earlier publication (1952) already referred to, it has been shown that there is a difference in the transmission of sound through granite and limestone. This difference is intimately connected with granular structure, and variation of mineralogical composition from grain to grain. In order to eliminate the effect of mineralogical composition and study the effect of granular structure alone, in the present investigation, three quartzites and three limestones which are for all practical purposes monomineralic, have been chosen. From the microphotographs of the three quartzites (Fig. 1) it is at once clear that grain size varies in the three rock sections in an increasing order. This observation put together with ultrasonic velocities given in Table I makes it quite evident that ultrasonic velocities, both longitudinal and torsional, decrease with increasing grain size. The microphotographs in Fig. 2 of the limestone also confirm the above result. It may further be recorded here that the intensity of the sound beam, is greatly reduced during transmission through coarse grained quartzite No. 3 in comparison with that in the fine grained quartzite No. 1. Limestones Nos. 4 and 6 show the same result. Thus, coarseness of grain in a rock not only makes the sound beam traverse slower but also weakens it to a great extent.

4. Summary and Conclusion

Ultrasonic velocities, in monomineralic rocks like Quartzites and Limestones, are determined using the total internal reflection method. In coarse

grained rocks, the velocities are low and the absorption is high. In fine grained rocks, the velocities are high and the absorption low.

In conclusion, the author desires to express his grateful thanks to Professor S. Bhagavantam for his kind guidance and interest shown throughout this investigation.

REFERENCES

1. Balakrishna, S. .. *Curr. Sci.*, 1952, **21**, 241.
2. Krishnamurthi, M. and Balakrishna, S. .. *Proc. Ind. Acad. Sci.*, 1953, **38**, 495.
3. Mason, W. P. and Mcskimin, H. J. .. *J. Acoust. Socie. Amer.*, 1947, **19**, 365.
4. Takahashi and Yasusato .. *Bull. Earth Quake Res. Inst.*, 1949.

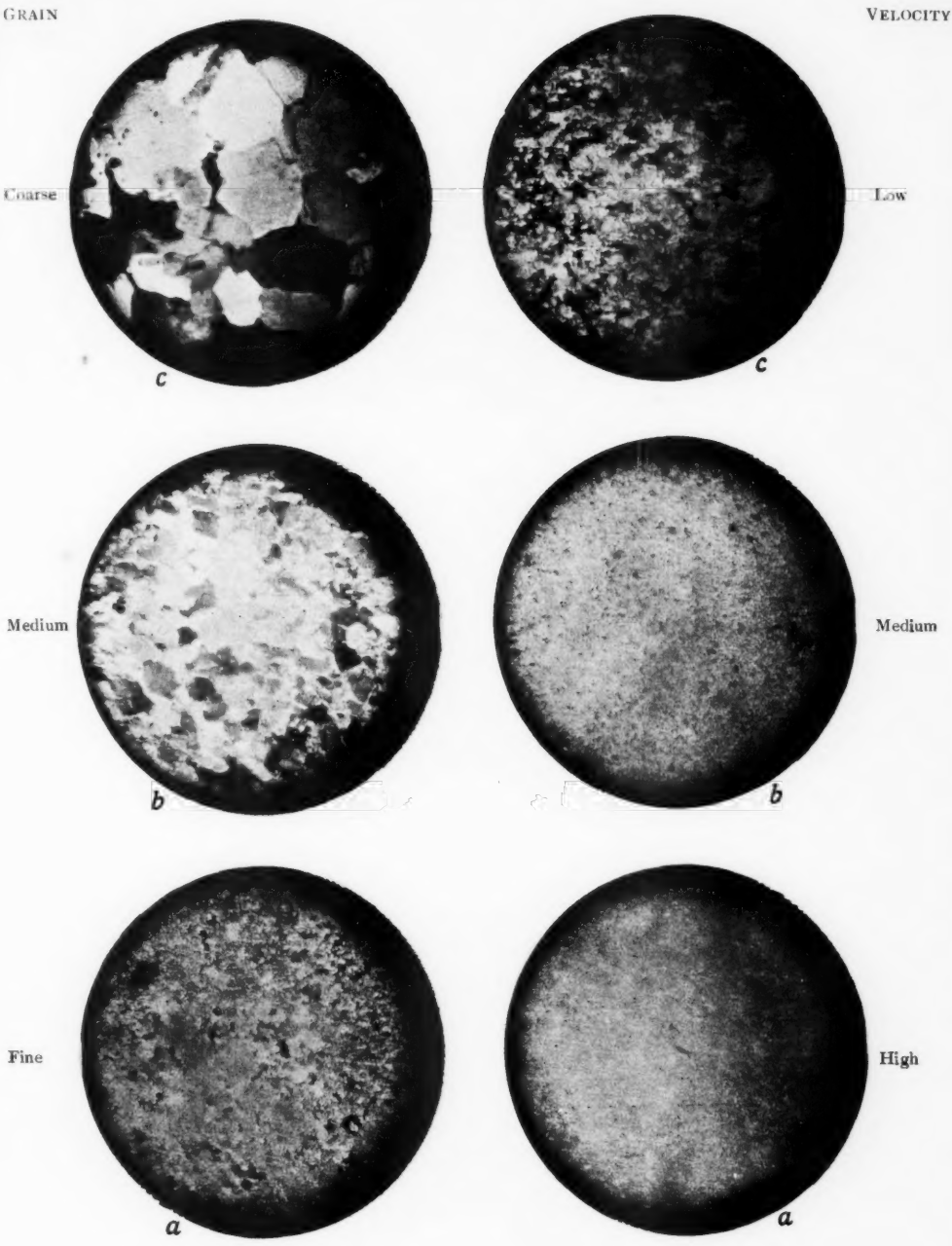

FIG. 1. Quartzites

FIG. 2. Limestones

Magnification : ×30

NUCLEAR INTERACTIONS OF K-MESONS

By R. R. Daniel and D. Lal

(*Tata Institute of Fundamental Research, Bombay* 1)

Received December 6, 1954

(Communicated by Prof. Bernard Peters, F.A.SC.)

Abstract

Fast K-mesons (τ- as well as K_π-mesons) with energies between 150 and 250 MeV can cause nuclear disintegrations and lose a substantial fraction of their kinetic energy without losing their identity. The character of the interaction in three of the four cases discussed here exhibit a remarkable degree of similarity.

The nuclear capture of a K-meson at rest is discussed. The nature and distribution of prongs in the capture star suggest that a Λ°-hyperon may have been formed during the capture process.

I. Introduction

During recent investigations with large emulsion block detectors[1] exposed to cosmic radiation at high altitude, we have observed examples of the interaction of fast K-mesons with nuclei and have also obtained some additional information on the interaction of negative K-mesons at rest. In this paper we describe five events:

(*a*) three have been interpreted as nuclear interactions of fast K-mesons,

(*b*) one event can be attributed either to Coulomb or to nuclear interaction of a K-meson, and

(*c*) one represents an example of a negative K-meson which gives rise to an unusual capture star when at rest.

For the sake of convenience and completeness in describing the available information on these events, we have adopted the following conventions. The tracks are classified as white, grey or black as given in Table I. This is,

Table I

Type of track	Symbol	Grain density interval
White	w	$g < 1{\cdot}5\, g_{pl}$*
Grey	g	$1{\cdot}5\, g_{pl} < g < 4\, g_{pl}$
Black	b	$g > 4\, g_{pl}$

* g_{pl} is the grain density at the plateau of the ionization curve as measured by grain counting tracks of fast electron-positron pairs.

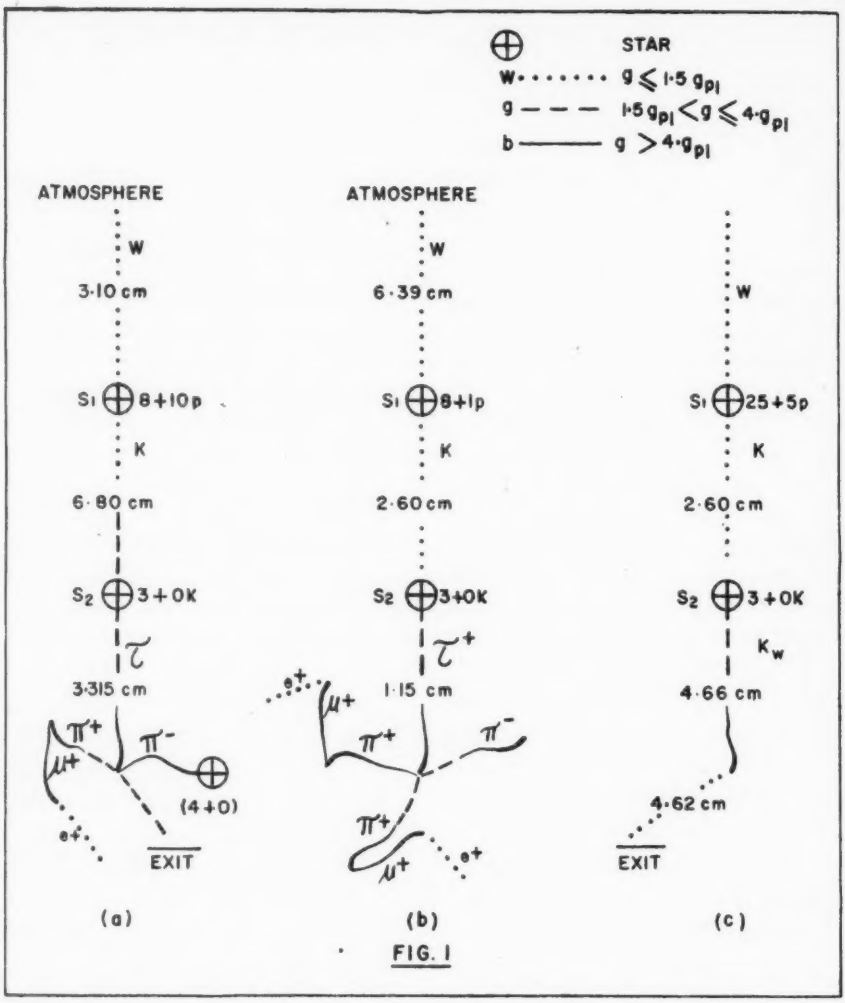

FIG. 1

therefore, a classification of particles according to specific ionisation irrespective of mass and charge.

If the *mass* of the particle is known, the symbols L, K and Y, with their conventional meanings,[2] are used. If in addition the *exact decay scheme* is known, the particle is designated by its Greek letter (μ, π, τ, Λ, etc.). If the decay process cannot be completely described, we add the available

information on the decay process as subscript. With these conventions, we designate a K-meson disintegration into a relativistic singly charged particle as K_w and if the identity of this charged decay product is established as electron, μ-meson or π-meson, the parent particle is designated as K_e, K_μ or K_π respectively.† When the particle produces a capture star at the end of its range, the subscript σ will be used.

II. Nuclear Interactions of Fast K-Mesons

In the course of tracing stopped K-mesons to the point of their creation, we have observed three events which exhibit similar features. Schematic diagrams of these are given in Fig. 1. A relativistic singly charged particle enters the stack of emulsions (Figs. 1 *a* and 1 *b*) and produces a high energy nuclear disintegration S_1. In each case one of the fast particles emerging from S_1 is shown to be a K-meson and causes a second star S_2, from which a τ-meson is emitted. Fig. 1 *c* shows a very similar event in which the primary was not traced to its entrance point in the stack; here, however, we are dealing with a different type of K-meson designated as K_w. As indicated in the figures, the chain of events extends over a distance of about 10 cm. which is of the order of the dimensions of the emulsion blocks used ($12\times15\times15$ cm. and $8\times15\times15$ cm.). Measurements made on the three S_1 and S_2 stars and on the particles which connect them will now be described.

(1) *The Primary Stars* S_1 *and the Interconnecting Particles*

In Table II, we have listed the measurements made on the S_1 stars and the interconnecting particles.

It is apparent from the observed grain densities of the tracks produced by the interconnecting particles, that they are non-relativistic and singly charged and do not have enough energy to *produce* the S_1 stars. Therefore, they are *emitted* from S_1 and caused the S_2 stars.

All the tracks of secondary particles associated with the S_1 stars with grain density $g > 1{\cdot}2\, g_{pl}$ were followed until they left the stack or were brought to rest. We did not find any other unstable particle decaying in flight or at rest while in the stack. One grey track in event No. 1 stopped suddenly in the middle of the emulsion without showing the usual increase in grain density or scattering and without giving rise to any charged particle.

† Our nomenclature differs, therefore, from that used by Gregory *et al.*[3] These authors designate K_μ as a particle which emits a μ-meson in a *two body* decay process, while in our system, K_μ implies only that the charged decay product was identified as μ-meson.

TABLE II

Event No.	Parent Star S_1	Tracks in Star S_1		Interconnector $S_1 - S_2$			
		Tracks	Fate	Total obs. Range	Av. length per plate	Grain density near S_1 star g/g_{pl}	Grain density near S_2 star g/g_{pl}
1	8+10 p	Primary	Enters stack				
		9 whites	Not traced				
		1 white	Interconnector	6·80 cm.	1·305 mm.	1·43 ± ·055	1·67 ± ·055
		3 greys	Leave stack				
		1 grey	Suddenly stops in middle of emulsion				
		4 blacks	End				
2	8+1 p	Primary	Enters stack				
		1 white	Interconnector	2·60 cm.	2·10 mm.	Average Grain Density = 1·285 ± ·055	
		1 gre	Ends				
		7 blacks	End				
3	25+5 p	Primary	Not traced				
		4 whites	Not traced				
		1 white	Interconnector	2·60 cm.	1·625 mm.	Average Grain Density = 1·35 ± ·055	
		8 greys	Leave stack				
		2 greys	Interact				
		5 greys	End				
		10 blacks	End				

(2) *The Secondary Stars S_2*

The observations made on the S_2 stars are listed in Table III.

It may be of interest to note that in each S_2-star there are only three secondary tracks, one K-meson, one recoil and one black prong which in all cases looks heavier than a proton although the track lengths are insufficient to make a reliable mass measurement. All these particles were brought to rest in the stack.

(3) *Identification of the Interconnecting Particles*

As mentioned earlier the interconnecting particles move towards the S_2-stars each of which emits a K-meson. We can show that in all the three examples, the interconnecting particle itself must be a K-meson.

TABLE III

Event No.	S_2 Star	Tracks in Star S_2			Energy loss suffered by the inter-connector in MeV.	Angle between the Inter-connector and the K-meson
		Range	Identity	Kinetic Energy in MeV.		
1	3+0K	6·80 cm.	Interconnector (assumed mass 965 m_e)	148		
		1·315 cm.	τ-meson*	47	101	78°
		836μ	Probably deuteron	17		
		2·4μ	Recoil	..		
2	3+0K	2·60 cm.	Interconnector (assumed mass 965 m_e)	246		
		1·15 cm.	τ^+-meson*	44	202	38°
		45μ	Probably deuteron	2·8		
		2·0μ	Recoil	..		
3	3+0K	2·60 cm.	Interconnector (assumed mass 965 m_e)	219		
		4·66 cm.	K_μ-meson †(assumed mass 965 m_e)	102	117	105·5°
		2000μ	Probably dueteron	28		
		1·6μ	Recoil	..		

* All but one of the decay products of the two τ-mesons come to rest in the stack; the τ-mesons suffer the normal decay into three π-mesons. Q-values and other details will be reported separately.

† The decay track of K_μ leaves the stack after traversing 4·62 cm. and has an average length of 3·56 mm. per plate. Its grain density is 0·975 ± ·04 and $p\beta = 150 \pm 16$ MeV./c. One could, therefore, identify this K-meson with the $\theta^\pm$ - meson:

$$\theta^\pm \rightarrow \pi^\pm + \pi^0$$

and

$$M_{\theta^\pm} = M_\tau = 965\, m_e.$$

Firstly, it is clear that they cannot be L-mesons because L-mesons of comparable initial velocity will exhibit much larger changes of grain density in traversing comparable distances. Therefore, considering only known particles, we are left with the following possibilities. The inter-connecting particles are:

(*a*) protons, hyperons, deuterons or tritons, or

(*b*) they are K-mesons.

Let us take the first alternative. From each S_2-star an identified K-meson is emitted; the collision between a proton, deuteron or triton and a nucleon in the target nucleus must, therefore, result in the creation of a K-meson. We now consider whether for the observed velocities of the interconnecting particles there is sufficient energy available to create a K-meson of mass 965 m_e at rest in the centre of mass system of the incoming particle (proton, deuteron or triton) and a nucleon in the target nucleus. In order to decrease the energy requirement to its lowest possible value we assume that the nucleon which was struck had a kinetic energy of ~ 20 MeV inside the target nucleus and that its direction of motion was such as to meet the incident particle head-on. (We assume here that the K-meson is created in a single collision between one of the nucleons of the incident deuteron or triton and one nucleon of the target nucleus.) In Table IV we give the calculated threshold energies for the production of a K-meson by a proton, deuteron or triton in such collisions and compare them with the energies estimated from the observed grain densities of the three interconnecting particles.

TABLE IV

Assumed incident particle	Proton	Deuteron	Triton
Threshold energy to produce a K-meson of mass 965 m_e	790 MeV.	1400 MeV.	1775 MeV.
Kinetic energy of interconnector from the observed grain density			
Event No. 1	262±15 MeV.	524±30 MeV.	786±45 MeV.
No. 2	384±18 MeV.	768±36 MeV.	1152±54 MeV.
No. 3	354±18 MeV.	708±36 MeV.	1062±54 MeV.

It is apparent from Table IV that in none of the three events, the energy available in the C.M. system of the colliding particles is sufficient to create a K-meson. Therefore, in each case the interconnecting particle itself must be a K-meson. We have also made direct mass measurements on the interconnecting tracks; as shown below the results are consistent with this conclusion.

(4) *Direct Mass Measurements on the Interconnecting Tracks*

(*a*) *Variation of Grain Density along the Track of the Interconnecting Particles.*—Event No. 1 is the only case where a significant increase in grain density along the track of the interconnector is observed (Table II). The grain densities measured near the stars S_1 and S_2 are $1{\cdot}43 \pm 0{\cdot}055$ and $1{\cdot}67 \pm 0{\cdot}055$ respectively. The observed increase in grain density after a

length of 6·1 cm. corresponds to a particle of mass 800–2300 m_e. The other two interconnectors do not show any significant increase in the grain density, nor do we expect such increase in the observed amounts of absorber traversed if the particles are K-mesons.

(*b*) *Scattering* versus *Grain Density*.—As is seen from Table II, although the total track lengths available for measurements are large, the average lengths per plate of the interconnectors are 1·305, 2·1 and 1·625 mm. only. At energies with which we are dealing here and for the observed steepness of their tracks the emulsion distortion becomes very important and measurements of coulomb scattering become unreliable. For the slowest interconnecting particle we obtained from scattering a mass value of 820 $\pm$ 180 m_e after making distortion correction using higher order differences.[13] In the other two cases we obtained mass values $\sim$ 500 m_e. Though these values are not very reliable, they are not inconsistent with other findings.

(5) *Interpretation of the Events*

We have shown in the previous section that in all these events the interconnectors are fast K-mesons which cause the S_2-stars and from each S_2-star a τ or K_w is ejected. The events, therefore, represent nuclear interactions of fast K-mesons. If we assume that the interconnecting K-mesons are of the same type as those emerging from their interaction stars, we may infer that τ and K_w-mesons interact strongly with nuclear matter and that their structure is such that they can retain their identity in collisions where energies upto $\sim$ 200 MeV. are exchanged, that is, energies larger than the rest mass of π-mesons.

It must, however, be pointed out, that since these events were discovered by tracing K-mesons backward from the point at which they came to rest, events in which fast K-mesons interact, and lose their identity in the process would not have been discovered in our investigation.

(6) *A Fourth Possible Case*

A particle is emitted from a star of the type 13 + 1*n*. After a traversal of 5·66 mm. of emulsion, the track suffers a deflection of 138°. After an additional 6·25 mm. the particle comes to rest, and emits a relativistic secondary. Scattering measurements on the track before and after the deflection show that the mass values obtained for both the sections is $\sim$ 1000 m_e. Therefore, in our nomenclature the track is designated as a K_w-meson. The grain density and scattering measurements show that the energy loss is of the order of a few MeV. only. At the point of deflection, there is a short track, very likely due to a recoiling nucleus. The event

could, therefore, be interpreted either as a nuclear scattering or as a coulomb scattering of a K_w-meson by a heavy atom in the emulsion.

III. CAPTURE OF A NEGATIVE K-MESON AT REST

We have previously reported[4] nuclear interactions of negative K-mesons at rest. We have now observed an additional case which has some peculiar, though possibly accidental, characteristics. A K-meson is ejected from a nuclear disintegration of the type $7 + 8\,p$ and brought to rest in the same emulsion giving rise to a capture star. Details of measurements made on the K^--meson, its parent star and the capture star are given in Table V.

TABLE V

Present Star	Range of K^-	Mass of K^- from Range *vs.* Scattering	Capture Star				
				Total Range	Av. length/ plate	Identity	Kinetic Energy
$7+8\,p$	2·9 mm. (in one plate)	$1040 \pm 200\ m_e$	1	2·833 cm.	1·18 mm.	π^--meson	44·4 MeV.
			2	1·734 cm.	5·78 mm.	Proton	74·3 MeV.
			3	2·7μ	..	Recoil	..

The mass of particle (2) emitted from the capture star was estimated from scattering measurements using the constant sagitta method[5] and found to be $2400 \pm 500\ m_e$. Since there is no visible decay product emerging from the end of the track and since the scattering measurements are not inconsistent with its being due to a proton, we assume that this track was in fact produced by a proton.

The curious thing about this capture star is the fact that, if we analyse it on the assumption that the proton and the π^--meson arise from the decay of a neutral particle, we find that the Q-value is $36{\cdot}7 \pm 0{\cdot}9$ MeV., which is very close to the Q-value $37{\cdot}40 \pm {\cdot}27$ MeV. of the Λ° hyperon.[6] (The angle included between the two tracks is 70·8°.) The event could, therefore, be interpreted in two ways:

(*a*) The three observed quantities, namely, the π^--meson range, the proton range and the angle between their trajectories are such that the apparent Q-value happens to come close to the Q-value of Λ° by accident and the event does *not* represent the decay of a Λ°.

(*b*) The event represents the production of a Λ° during the capture of a K^--meson and the Λ° decayed either at the point of creation or within a small distance of the order $\lesssim 1\,\mu$.

Purely on life-time considerations ($\tau_{\Lambda^0} = 3 \cdot 7 \times 10^{-10}$ sec.)[7] the second alternative seems quite unlikely. Still the close coincidence of "Q-values' seems remarkable.

Evidence for the association of K-mesons and hyperons in production was given in an earlier paper,[4] similar observations were later reported by other workers.[8,9] The close connection which seems to exist was firmly established by the experiments of Fowler *et al.*[10] who used artificially produced π^--mesons traversing a diffusion cloud chamber filled with hydrogen. These results can be represented in the general form:

$$\pi + \mathscr{N} \rightarrow \Lambda + \mathrm{K}, \tag{1}$$

where the symbol $\mathscr{N}$ designates a nucleon. The genoa Group[11] using emulsions and DeStaebler[12] using cloud chamber have shown that charged or neutral hyperons can be associated with the capture of negative K-mesons. The process could perhaps be written:

$$\mathrm{K} + \mathscr{N} \rightarrow \Lambda + \pi, \tag{2}$$

The example obtained by the Genoa group and one of the cases reported by DeStaebler could then be written down as particular cases of eq. (2):

$$\mathrm{K}^- + \mathscr{N}^\circ \rightarrow \Lambda^- + \pi^\circ, \tag{2a}$$

and

$$\mathrm{K}^- + \mathscr{N}^\circ \rightarrow \Lambda^\circ + \pi^-, \tag{2b}$$

respectively. Two other events observed by DeStaebler and probably the one reported here are other particular cases of eq. (2), namely:

$$\mathrm{K}^- + \mathscr{N}^+ \rightarrow \Lambda^\circ + \pi^\circ, \tag{2c}$$

(Energy and momentum distribution of the visible fragments in our event are consistent with this scheme.)

IV. Acknowledgement

We are deeply indebted to Professor B. Peters for valuable discussions and keen interest in this work.

We would like to express our thanks to Miss Purohit who discovered the K^--event.

References

1. Daniel, R. R., Friedmann, G., Lal, D., Yash Pal and Peters, B. *Proc. Ind. Acad. Sci.*, 1954, **40A**, 151.
2. Amaldi, E., Anderson, C. D., Blackett, P. M. S., Fretter, W. B., Leprince-Ringuet, L., Peters, B., Powell, C. F., Rochester, G. D., Rossi, B. and Thomson, R. W. *Nature*, 1954, **173**, 123.

3. Gregory, B., Lagarrigue, A., Leprince-Ringuet, L., Muller, F. and Peyrou, Ch. *Nuovo Cimento*, 1954, **11**, 292.
4. Lal, D., Yash Pal and Peters, B. .. *Phys. Rev.*, 1953, **92**, 438.
5. Biswas, S., George, E. C. and Peters, B. .. *Proc. Ind. Acad. Sci.*, 1953, **38A**, 418.
6. This value is derived from the most favourable cases of Λ°-decays observed in this laboratory to date.
7. Page, D. I. .. *Phil. Mag.*, 1954, **45**, 863.
8. Castagnoli, C., Cortini, G. and Manfredini, A. *Nuovo Cimento*, 1954, **12**, 464.
9. Dahanayake, C., Francois, P. E., Fujimoto, Y. Iredale, P., Waddington, C. J. and Yasin, M. *Phil. Mag.*, 1954, **45**, 855.
10. Fowler, W. B., Shutt, R. P., Thorndike, M. and Whittemore, W. L. *Phys. Rev.*, 1954, **93**, 861.
11. Reported by the Genoa Group at the Padova Conference, 1954.
12. DeStaebler, H. .. *Phys. Rev.*, 1954, **95**, 1110.
13. Biswas, S., George, E. C., Peters, B. and Swamy, M. S. Reported at the Padova Conference, 1954.

REFRACTION OF LIGHT IN SOLIDS BY ULTRASONIC WAVES

By K. S. Iyengar

(From the Physical Laboratories, Osmania University, Hyderabad, India)

Received December 18, 1954

(Communicated by Dr. S. Bhagavantam, F.A.SC.)

1. Introduction

The refraction of a narrow beam of light in a sound field was first observed by Lucas and Biquard (1932). They described it as a broadening effect of the slit image. Hueter and Pohlman (1949) used this effect for the measurement of absorption of ultrasonic waves. Recently Kolb and Loeber (1954) have employed it for finding the pressure distribution in a stationary sound wave. All these workers used liquid media for their studies. The purpose of this paper is to describe the effect in solids.

2. Experimental Arrangement

The experimental set-up employed by the author for observing the broadening, is similar to the one described by Kolb and Loeber (1954). Instead of the liquid cell of their experiment, a rectangular block of a transparent solid, suitably mounted on an X cut transducer, is placed immediately behind a narrow adjustable slit. A convergent lens of about 20 cm. focal length forms a sharp image of the slit on a screen placed at a distance of 2 to 3 metres. The transducer is excited at one of its harmonics.

The effects described here have been observed at a frequency of 2·63 MC/S.

3. Estimation of Maximum Change of Refractive Index in Amorphous Solids

If a stationary ultrasonic field of wavelength λ is set up in an amorphous solid, the refractive index n_x at a distance x is given by

$$n_x = \frac{n + \mu \sin 2\pi x}{\lambda}, \qquad (1)$$

where n is the refractive index of the undisturbed solid and μ the maximum change in the refractive index. A ray of light on traversing the sound field

in a perpendicular direction will get deflected by an amount S on the screen where

$$S = \frac{a\delta dn_x}{dx} \tag{2}$$

a is the distance of the screen from the lens and δ the width of the sound field. Substituting for dn_x/dx from (1)

$$S = \frac{2\pi a\delta\mu}{\lambda} \cdot \frac{\cos 2\pi x}{\lambda}$$

is obtained. Since an amorphous solid becomes doubly refracting under strain, the indices of refraction in the parallel and perpendicular directions of strain will be different. If they are denoted by μ_1 and μ_2, the deflections will be different according as the ray of light is polarised in a parallel or perpendicular direction, and will be related to each other in the ratio

$$\frac{S_1}{S_2} = \frac{\mu_1}{\mu_2} \tag{3}$$

The maximum deflections in the two directions are given by

$$S_{1\max.} = \frac{2\pi a\delta\mu_1}{\lambda} \text{ and } S_{2\max.} = \frac{2\pi a\delta\mu_2}{\lambda}$$

These will occur when the ray is passing very close to a node. A photograph of the broadening of the slit image for one of the optical glasses is shown in Fig. 1. A double-image prism was used to obtain the two images shown at (*a*) and (*b*). Using sodium light, the broadening observed $2\,S_{1\max.}$ and $2\,S_{2\max.}$ were ·8 mm. and 1·1 mm. respectively when the screen was 230 cm. from the lens. With $\delta = 1 \cdot 30$ cm. and $\lambda = \cdot 161$ cm. the calculated values of μ_1 and μ_2 are $3 \cdot 43 \times 10^{-6}$ and $4 \cdot 71 \times 10^{-6}$ respectively.

4. Determination of the Ratio of the Strain-Optical Constants

The broadening effect also enables the determination of the ratio of strain-optical constants of amorphous solids. Consider a plane sound wave of angular frequency ω and velocity v, to be travelling in the solid in the x direction. The elastic displacement is given by the expressions

$u_x = A \cos \omega t \cos \omega x/v$ for a longitudinal wave and

$u_y = B \cos \omega t \cos \omega x/v$ for a transverse wave.

The strains thus set up have components $xx = du_x/dx$, $yy = du_y/dy$ and $xy = du_x/dy + du_y/dx$.

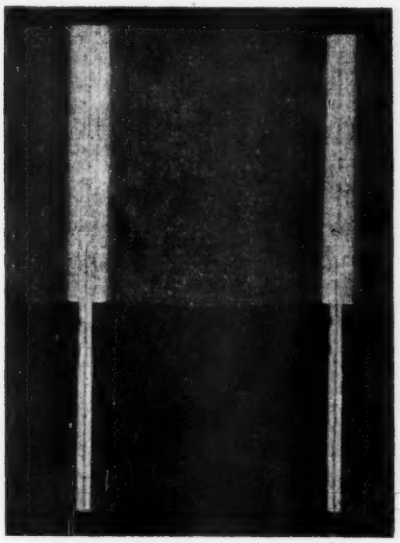

a *b*

FIG. 1. The Lucas-Biquard effect in glass

(*a*) Light polarised perpendicular to the sound wave

(*b*) Light polarised parallel to the sound wave

The displacements and strains in the z direction are omitted because they will have no influence on light travelling in that direction. Under the influence of these strains every volume element of the solid will become birefringent. The section perpendicular to the z direction is characterised by the index

$$B_{11}x^2 + B_{22}y^2 + 2B_{12}xy = 1 \tag{4}$$

ellipse where the B's are the polarisation constants.

In the theory of photoelasticity it is assumed that the divergence between the coefficients of the modified and the original index ellipsoids are small quantities of the first order in strains.

$$\begin{aligned} B_{11} - B &= P_{11}xx + P_{12}yy \\ B_{22} - B &= P_{12}xx + P_{11}yy \\ B_{12} &= P_{44}xy \end{aligned} \tag{5}$$

The P's are the strain-optical constants and $P_{44} = (P_{11} - P_{12})/2$. The principal axes of the ellipse (4) are tilted at an angle θ with respect to the co-ordinate axes where

$$\tan 2\theta = \frac{2B_{12}}{(B_{11} - B_{22})}$$

For longitudinal waves xy and yy are zero and θ is zero. Eq. (4) reduces to

$$B_{11}x^2 + B_{22}y^2 = 1.$$

If μ_1 and μ_2 are the changes in refractive index in the x and y directions respectively

$$B_{11} = \frac{1}{(n + \mu_1)^2} = \frac{1}{n^2} - \frac{2\mu_1}{n^3}$$

and

$$B_{22} = \frac{1}{(n + \mu_2)^2} = \frac{1}{n^2} - \frac{2\mu_2}{n^3}$$

Substitution of these values in (5) gives

$$\frac{\mu_1}{\mu_2} = \frac{P_{11}}{P_{12}} \tag{6}$$

For a transverse wave θ is 45° and if the changes of refractive index are considered in the direction of the principal axes the corresponding expression comes out as $\mu_1/\mu_2 = -P_{44}/P_{44} = -1$. Eqs. (3) and (6) together give

$$\frac{P_{11}}{P_{12}} = \frac{S_1}{S_2} \tag{7}$$

In Table I this ratio is given for two optical glasses. It is determined for three wavelengths of light. These ratios have been verified by other photoelastic methods (Mueller, 1938; Ramachandran, 1947).

TABLE I

The ratio of strain-optical constants in glasses for three wavelengths of light

Glass	P_{12}/P_{11}		
	5893 Å	5461 Å	4358 Å
I	$1{\cdot}3_7$	$1{\cdot}3_8$	$1{\cdot}4_0$
II	$1{\cdot}5_4$	$1{\cdot}5_2$	$1{\cdot}5_7$

The foregoing arguments are valid for crystalline media also. It can be shown that in the case of cubic crystals the ratios P_{11}/P_{12} and $(P_{11}+P_{12})/P_{44}$ for the $T_d O$ and O_h classes, and P_{11}/P_{12} and P_{11}/P_{13} for T and T_h classes are obtained by considering prisms of suitable cuts properly oriented with respect to the direction of light.

5. Velocity of Sound in Solids

As in the case of liquids, the broadening effect enables the determination of the velocity of sound in solids. As the solid is moved parallel to the direction of the sound-wave, opposite the slit, the image narrows and broadens periodically. By measuring the displacement of the solid for a given number of maxima or minima the wavelength of the sound-wave is determined. The velocity of longitudinal waves thus determined in two glasses, are given in column 1 of Table II. In column 2 the values of velocities as obtained by the diffraction method are recorded. It will be seen that there is a close agreement between the two values.

Table II

Velocity of longitudinal sound waves in glasses as measured by (1) the broadening effect, (2) the diffraction method

Glass	v_1 KM/S	
	1	2
I	4·23	4·220
II	4·49	4·478

6. Summary

The Lucas-Biquard effect of optical refraction in a sound field is experimentally studied in glasses. It is shown that the effect enables the determination of the absolute changes of refractive index, the ratio of elasto-optical constants and the elastic constants of amorphous and crystalline solids.

The author is grateful to Prof. S. Bhagavantam for his interest in this work.

References

1. Hueter, T. and Pohlman, R. .. *Z. angew. phys.*, 1949, **1**, 405.
2. Kolb, J. and Loeber, A. P. .. *J. Acoust. Soc. Am.*, 1945, **26**, 249.
3. Lucas, R. and Biquard, P. .. *J. Phys. radium*, 1932, **3** (7), 464.
4. Mueller, H. .. *Zeit. f. Krist.*, 1938, **99A**, 122.
5. Ramachandran, G. N. .. *Proc. Ind. Acad. Sci.*, 1947, **25**, 208.

EVIDENCE FOR THE CHARGED θ-MESON

By M. V. K. Appa Rao and S. Mitra
(*Tata Institute of Fundamental Research, Bombay* 1)

Received January 13, 1955
(Communicated by Dr. B. Peters, F.A.SC.)

Abstract

A K-meson is found to decay at rest into a nearly relativistic secondary particle. The secondary particle produces a nuclear disintegration in flight and is identified as a π-meson of kinetic energy ~ 110 MeV. The event is interpreted as the decay of a $\theta^{\pm}$-meson according to the scheme:

$$\theta^{\pm} \rightarrow \pi^{\pm} + \pi^{0} + (222 \pm 12 \text{ MeV.})$$

1. Introduction

Particles which come to rest by ionization and then emit a charged L-meson have been observed by many laboratories during the last two years. Heavy K-mesons as well as hyperons occur as parent particles and both π- and μ-mesons as daughter products. One particular type of particle, a charged K-meson decaying into one charged and one neutral π-meson:

$$\theta^{\pm} \rightarrow \pi^{\pm} + \pi^{0} \qquad (1)$$

has been suggested by Powell (Copenhagen Conference). Evidence has been accumulating in favour of the existence of this particle, but conclusive proof is still lacking.

In cloud chambers, there are several events in which a particle comes to rest and emits a secondary whose range is close to 60 gm./cm.^{2} of lead (corresponding to the expected energy of $\pi^{\pm}$-meson from $\theta^{\pm}$ decay); sometimes a soft cascade accompanies the decay. But in none of these cases could the primary or the secondary particle, through mass measurements, be directly identified as K-meson and π-meson respectively.

In nuclear emulsions many events have been reported in which the primary is identified as a K-meson and the secondary as a L-meson. In some cases the L-meson seems to carry about 50% of the available energy suggesting a two-body decay. The neutral π-meson assumed to be emitted by the $\theta^{\pm}$-meson is not observable at present except through pair production

induced by the γ-rays into which it decays. In nuclear emulsions, the electron-positron pairs are observable, but since they are usually separated from the decay point by a distance of several centimetres, it will only in rare cases be possible to associate a given electron-positron pair with the decay of a heavy particle. Nevertheless, the identification of the charged θ-meson in emulsions is possible, provided the charged decay product can be definitely identified as a π-meson and provided it can be shown that its total energy E_π and the mass of the parent particle are connected by the relation appropriate to decay scheme (1) namely:

$$M_{\theta^\pm} = E_{\pi^\pm} + (E^2_{\pi^\pm} + m^2_{\pi^0} - m^2_{\pi^\pm})^{\frac{1}{2}} \qquad (2)$$

Several such cases in emulsions have been reported. In each case the secondary meson is, however, identified as a π-meson only by measurement of ionization and scattering, which is never quite conclusive. In the event reported here the secondary is observed to interact with a nucleus and, therefore, can definitely be identified as a π-meson.

Since there is not yet conclusive evidence for the charged θ-meson which decays into two π-mesons, it still seems worthwhile to report individual cases which are easiest interpreted by such a decay scheme.

II. Description of the Event

A K-meson (K-15) is ejected from a star of type $16 + 0\,n$ and comes to rest after traversing 4·98 mm. in two emulsions. A fast charged particle is emitted from the point at which the K-meson comes to rest. The track of the secondary particle is very flat and has a potential range of ~ 10 cm. in the stack (size of the stack $15 \times 15 \times 12$ cm.^{3}).[1] However, after traversing a distance of 4·05 cm. in two emulsions it produces a nuclear disintegration of type $5 + 0\,p$.

III. Measurements

1. *Primary Particle.*—The scattering measurements on the primary particle track were made by the constant Sagitta method.[2] We obtain a mass

$$M = 937\ {}^{+250}_{-170}\ m_e$$

2. *Secondary Particle.*—Measurements of scattering and grain density were made on the secondary particle track.

(*a*) *Scattering Measurements.*—The region of the plate in which the decay occurs is distorted due to the formation of a bubble

during processing. Hence we restricted our scattering measurements to the second plate. Using a constant cell length of 50μ, second and third differences (d_2 and d_3) were evaluated for 50μ, 100μ and 150μ cells. The values for d_2 were calculated by eliminating noise with higher cell sizes and also by removing constant noise. The mean α_{100} was calculated and $p\beta$ was obtained. The results are given in Table I.

(*b*) *Grain Density Measurements.*—Grain density on the secondary particle track was measured in both the emulsions traversed by it. Elaborate grain density measurements were made on flat electron-positron pairs in the same plate to obtain the plateau value of grain density for the plate. Measurements of grain density on electron-positron pairs were restricted to the same depth from the emulsion surface as that of the secondary track.

The value for $p\beta$ obtained from scattering measurements and the g/g_{pl} obtained for the grain density show that the secondary particle must be an L-meson. Since the secondary particle produces a disintegration, it is a π-meson. Using the known π-meson mass we have determined the kinetic energy of the π-meson using our empirical range *versus* grain density calibration curve, and the semi-empirical range-energy relation suggested by Daniel, George and Peters.[3] The results are given in Table I.

However, when the grain densities are close to minimum the calibration curves are not reliable. Therefore, we have calculated the kinetic energy of the π-meson also from the theoretical relation between specific energy loss and particle energy, as given by J. Smith.[4] Assuming that in the region of interest here, where the grain density is close to its minimum value, it is proportional to specific energy loss, we have

$$\frac{\left(\frac{dE}{dX}\right)}{\left(\frac{dE}{dX}\right)_{min.}} = \frac{g}{g_{pl}} \times \frac{g_{pl}}{g_{min.}}$$

where g_{pl} and $g_{min.}$ are the grain densities at plateau and at minimum respectively. The value for $g_{pl}/g_{min.}$ according to Stiller and Shapiro[5] and Fleming and Lord[6] is $1 \cdot 14 \pm \cdot 03$. Using our measured value of g/g_{pl} we calculated $(dE/dX)/(dE/dX)_{min.}$ from the above formula and obtained the corresponding π-meson energy with the help of table given by Smith.

TABLE I

Type of measurement	Plate in which measurement was made	Mean distance from the decay point	$p\beta$	g/g_{pl}	Total estimated range of π-meson		Kinetic energy of π-meson	
					(i) Using our empirical grain density *versus* range curve	(ii) Using the theoretical relation between particle energy and specific energy loss	From (i)	From (ii)
Scattering	Second	3·29 cm.	144^{+16}_{-14}	..	$11{\cdot}34^{+1{\cdot}55}_{-1{\cdot}25}$ cm.		$112{\cdot}3^{+10{\cdot}2}_{-\ 8{\cdot}2}$ MeV.	
Grain density	First	0·398 cm.	..	$1{\cdot}138 \pm {\cdot}032$	$6{\cdot}35^{+{\cdot}55}_{-{\cdot}50}$ cm.		$76{\cdot}1^{+\ 4{\cdot}4}_{-\ 4{\cdot}0}$ MeV.	
Grain density	Second	3·265 cm.	..	$1{\cdot}078 \pm {\cdot}033$	$10{\cdot}5^{+1{\cdot}3}_{-1{\cdot}3}$ cm.	$11{\cdot}5^{+2{\cdot}5}_{-1{\cdot}6}$ cm.	$106{\cdot}7^{+8{\cdot}7}_{-8{\cdot}7}$ MeV.	$113{\cdot}2^{+16{\cdot}3}_{-10{\cdot}5}$ MeV.

The indicated errors in the energy of the π-meson obtained from grain density are standard deviations due to the finite number of grains counted and the probable error due to uncertainty in the grain density *versus* range curve. Possible errors in the range energy curve have not been taken into account.

We have no explanation for the high g/g_{pl} value obtained in the first plate except that a bubble at a distance of about 2 mm. from the event introduced some inhomogeneities in development. In the second plate, we have no such disturbance and since here the values of true range of the π-meson as obtained from the grain density and scattering measurements are consistent with each other, we shall accept them as reliable and are forced to reject the grain density measurements in the first plate.

In order to be consistent with all remaining determinations within one standard deviation the π-meson energy should lie between the limits $104{\cdot}1 < W_\pi < 115{\cdot}4$ MeV.

IV. INTERPRETATION

Since no charged particle other than one π-meson is associated with the rest-point of the K-meson, we interpret the event as due to the decay of a K-meson into a single charged secondary and one or more neutral particles, rather than the capture of negative K-meson. The energy of the π-meson exceeds 100 MeV. and is, therefore, much too high to permit the interpretation $\tau^\pm \rightarrow \pi^\pm + 2\pi^0$. Other three-body decay schemes with less massive neutral particles cannot, however, be ruled out. If interpreted as a two-body decay we have the following results:—

$$\theta^\pm \rightarrow \pi^\pm + \pi^0 \qquad M_{\theta^\pm} = 971 \pm 22 m_e$$

$$K^\pm \rightarrow \pi^\pm + \gamma \qquad M_K = 892 \pm 24\, m_e$$

Both mass values are consistent with that obtained from direct measurements. The mass obtained from the first scheme agrees also with the mass of the neutral θ-meson ($M_{\theta^0} = 965 \pm 10\, m_e$)[7] which decays into two-charged π-mesons.

Thus while the event discussed here does not constitute a complete proof for the existence of charged θ-mesons, the agreement between measured quantities is closest on the assumption that the charged θ-meson exists and decays according to the scheme:

$$\theta^\pm \rightarrow \pi^\pm + \pi^0 + (222 \pm 12 \text{ MeV.})$$

ACKNOWLEDGEMENT

We are grateful to Professor B. Peters for his keen interest and guidance throughout the preparation of this paper. Our thanks are due to Dr. R. R. Daniel for his active help during our work and to Mr. D. Lal for helpful discussions.

REFERENCES

1. Daniel, R. R., Friedmann, G. B., Lal, D., Yash Pal and Peters, B. — *Proc. Ind. Acad. Sci.*, 1954, **40**, 151.
2. Biswas, S., George, E. C. and Peters, B. — *Ibid.*, 1953, **38 A**, 418.
3. Daniel, R. R., George, E. C. and Peters, B. — *Ibid.* (In press).
4. Smith, J. .. — *Phys. Rev.*, 1947, **71**, 32.
5. Stiller, B. and Shapiro, M. M. .. — *Rochester Conference Report*, 1952.
6. Fleming, J. R. and Lord, J. J. .. — *Phys. Rev.*, 1953, **92**, 511.
7. Thompson, R. W., Burnwell, J. R., Cohn, H. O., Huggett, R. W. and Karzmark, C. J. — *Ibid.*, 1954, **95**, 661.

2-55 Printed at The Bangalore Press, Bangalore City, by C. Vasudeva Rao, Superintendent
and Published by The Indian Academy of Sciences, Bangalore.

NOTICE TO AUTHORS

Scientific papers intended for publication in the *Proceedings of the Indian Academy of Sciences* can be accepted only when they are communicated by a Fellow of the Academy whose duty shall be to satisfy himself that such communications are fit to be read at the Meeting of the Academy and published in its *Proceedings*.

Papers should not ordinarily exceed fifty pages of foolscap. MSS. should be either typewritten or written in legible hand on one side of the paper. All papers should be carefully revised by the authors and should be absolutely in final form for printing. Position for text-figures should be indicated. Each paper shall conclude with a critical summary not exceeding 350 words.

Drawings, diagrams or other illustrations should be made on larger scale (preferably) twice the size than the ones in which they are intended to appear. They should be done in Indian ink on bristol board with lettering in pencil. Scale of magnification of camera lucida tracings should be indicated by the side of drawings. In certain special cases arrangements will also be made for monochrome lithographic and other colour plates. Reduction of illustrations desired should be indicated in pencil. Appropriate legends should accompany all drawings. Names of authors are to be marked in pencil on the left-hand corner of drawing sheets. Photomicrographs should be securely mounted with colourless paste.

All tables, quotations and footnotes which will be set hereafter (beginning from Vol. I, No. 2) in types smaller than the text, should be typewritten on separate sheets and placed with the text in proper sequence. Footnotes should be numbered in Arabic numerals.

References to literature in the text should be given, whenever possible, in chronological order, only the names of authors and years of publication, in brackets, being given. They should be cited in full after the summary, the authors' names following in alphabetical order. Thus,

Name or Names of author; Name of Journal (abbreviation) with a single underline; Year of publication; Number of Volume with a double underline, and lastly page. The following would be a useful illustration:—

Bergmann and Stather . . . . . Z. Physiol. Chem., 1926, 152, 189.

Two copies of slip-proof and wherever possible, a page proof for final revision will be sent to authors. All corrections are best made on the slip-proof which should be transmitted to the Office of the Academy. All proof corrections involve heavy expenses which would be negligible if the papers are carefully revised by the authors before submission.

Authors will be supplied with reprints of their papers at cost price, if intimation is given at the time of returning the slip-proof.

Blocks appearing in the *Proceedings* will be available for purchase by their respective authors. Orders for the same should be sent along with the corrected proofs and in any case not later than one month after the date of publication of the paper. The price charged would be 25% of the actual cost of the blocks *plus* freight and despatching charges. If the blocks are reproduced in other journals or publications, due acknowledgment should be made in them to the *Proceedings*.

The original drawings and plates of blocks appearing in the *Proceedings* will be returned to such of the authors as may require them provided the cost of despatching such originals is borne by them.

CONTENTS

		PAGE
On the Optical Behaviour of Crypto-Crystalline Quartz	Sir C. V. Raman and A. Jayaraman	1
Raman Spectra of Borax, Kernite and Colemanite	D. Krishnamurti	7
Transmission of Ultrasonics Through Rocks	S. Balakrishna	12
Nuclear Interactions of K-Mesons	R. R. Daniel and D. Lal	15
Refraction of Light in Solids by Ultrasonic Waves	K. S. Iyengar	25
Evidence for the Charged θ-Meson	M. V. K. Appa Rao and S. Mitra	30